Two-Stage Deep Learning Technology Based Iris Recognition Methodology for Biometric Authorization

Cheng-Shun Hsiao, Chia-An Chang, and Chih-Peng Fan *

Department of Electrical Engineering, National Chung Hsing University, Taiwan
Email: lotus2460@gmail.com (C.-S.H.); s1004662@gmail.com (C.-A.C.); cpfan@dragon.nchu.edu.tw (C.-P.F.)
*Corresponding author

***Abstract*—In this study, the proposed iris recognition method uses the You Only Look Once (YOLO)-based deep learning algorithm with the procedure divided into two stages. After extraction of the iris and pupil from the images, the iris Region of Interest (ROI) is identified by the classifier. Iris localization, iris segmentation, and feature enhancement are three crucial processes when extracting the iris ROI, and they constitute the first stage. Iris localization is firstly discussed, and the three methods are proposed with the system performance analyzed from the perspective of both system safety and affordability. The main difference among these methods is their complexity. Iris segmentation is then introduced, and an experiment is conducted to evaluate system performance when images are preprocessed for inputs by different segmentation methods, including images with and without normalization. Normalization and its necessary or unnecessary role in identifying images with deep learning are then analyzed. Finally, an examination of how feature enhancement influences the results of the proposed method is outlined. For system safety analysis, the Equal Error Rate (EER) of the proposed design approaches near zero; for system affordability analysis, the accuracy of the proposed design can be up to 98%.**

***Keywords*—biometric recognition, iris identification, iris location, YOLOv4-tiny, deep learning**

I. Introduction

Biometric recognition systems [1, 2] identify human physiological features, such as the iris, sclera, finger vein, fingerprint, palm, or voice, and behavioral characteristics, such as a signature or walking posture. Among these studies [1, 2], the iris is the most representative form of biometric recognition because it is stable, highly unique, and difficult to falsify. According to relevant research, each individual has a different iris, even twins. Therefore, the iris is widely used in biometric recognition (Fig. 1), such as in access control systems and criminal investigations. The iris is an annular structure in the eye surrounding the black area of the pupil. The iris is formed by genes, providing each individual with a different iris texture. In addition to its genetic diversity, the iris remains stable throughout an individual's life and is therefore ideal for use in biometric recognition. With the development of technology and new trends in artificial intelligence, iris recognition systems based on deep learning have been proposed. The iris recognition system proposed herein relied on a classifier, an object detector, and semantic segmentation, with the classifier used in identification and the object detector and semantic segmentation employed to locate the iris.

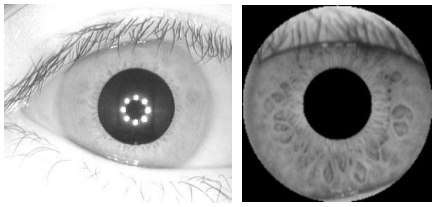

(a) (b)

Fig. 1. Eye images for iris recognition. (a) Original image (b) Iris ROI.

The iris recognition system architectures used in various studies are generally similar, and the first one was proposed by Daugman in 1993 [3]. The first method involves detection of the iris and sclera boundary using the integral and differential operator proposed by Daugman [3]. Hough transform is also widely used to locate the pupil and iris [4, 5], but ellipse fitting can detect the iris location with greater precision because the real shape of the iris is similar to an oval [6, 7]. Daugman proposed the rubber sheet model to normalize iris information with polar coordinates following iris segmentation. Many researchers have reported various methods of iris normalization based on Daugman's model, such as Qiaoli *et al*. [8] and Mohammed *et al*. [9]. To improve system accuracy, related images are being often further preprocessed after iris normalization. Common techniques such as the Gabor filter, histogram equalization, and Contrast Limited Adaptive Histogram Equalization (CLAHE) are widely applied to enhance iris features. The Gabor filter was adapted to extract specific frequency information in the images and is therefore suitable for texture extraction, and CLAHE was employed to enhance image contrast in [10]. Feature

Manuscript received May 23, 2023; revised July 6, 2023; accepted October 1, 2023; published February 15, 2024.

extraction algorithms of iris recognition systems include Scale-Invariant Feature Transform (SIFT) and Speeded-Up Robust Features (SURF) [10–12]. SURF is a modified version of SIFT and is several times faster than SIFT. The core function of these algorithms is to extract local features for computer vision, and this function has been applied in object recognition, image stitching and tracking the final step of an iris recognition system is identification. The Hamming distance, Euclidean distance, fast library for approximate nearest neighbors, and random sample consensus have been used in different studies. Koç and Uka [13] used a new feature extraction method and a new matching metric to find effective thresholds for separating the intra- and interclass distributions of iris images from different individuals using an 8-level quantization.

For iris recognition systems based on machine learning, the process focuses on iris identification, and Support Vector Machines (SVMs) are commonly used for such approaches. In Ref. [14, 15], iris features were extracted into vectors identified by SVM. Deep learning is typically employed for iris localization and identification. For iris localization, some researchers have located the iris region using semantic segmentation models, such as ISqEUNet [16], which localizes the iris region more completely than other approaches do. The input image of the model included both the NIR image and the visible image. The iris boundary and pupil mask were accurately detected using the deep multitask attention network-based iris segmentation model proposed by Wang *et al.* [17]. Neural network-based classifiers have been widely implemented for iris identification. In Ref. [18], the feature vector of the iris was identified using a shallow neural network, and Convolutional Neural Network (CNN)–based classifiers were also adopted for iris identification by Thuong *et al.* [19]. According to Ref. [20], capsule network architecture with a modified routing algorithm can be used for iris identification. In Ref. [21], the Modified-GLCM method was used to extract iris features and propose an algorithm to detect iris presentation attacks in combination with Multi-Layer Perceptron (MLP) networks, and it was used for iris recognition systems to detect attacks from wearing colored contact lenses.

In this study, for the iris recognition system, an iris image was first obtained through iris localization, and the iris segmentation method was employed. Optional feature enhancement could be used for the classifier, which then identifies a person based on the use of EfficentNet. The classifier predicted a probability for each corresponding class, and the class with the highest probability was designated as a prediction when this probability was higher than the threshold. This person was regarded as an intruder when the highest probability was lower than the threshold. The main contributions of this study are:

(1) For iris localization, the semantic segmentation models located the iris with more precision than other models but were more time-consuming. The applied YOLO-based model provides faster object detection to determine the iris location with noises and within a relatively short time.
(2) For iris segmentation, iris normalization was optional when it was implemented in the iris recognition system with the classifier based on deep learning.
(3) The iris recognition system became more stable when the pupil information and background were removed from the images.
(4) By experiments, images without feature enhancement achieved the best results, indicating that feature enhancement is optional for the classifier.

The rest of the study is stated as follows: In Section II, the previous works for iris recognition are described. The proposed two-stage iris recognition method by using YOLO-based deep learning iris location are presented in Section III. In Section IV, the experimental results and comparisons are revealed. Finally, the conclusion is stated in Section V.

II. Previous Works

A. Iris Recognition System

The workflow of most traditional iris recognition systems [3–12] can be split into the following steps: iris localization, segmentation, normalization, feature enhancement, feature extraction, and identification. To increase system performance, evaluation index estimation and more complex methods were proposed. Fig. 2 describes the flow of the general iris recognition system.

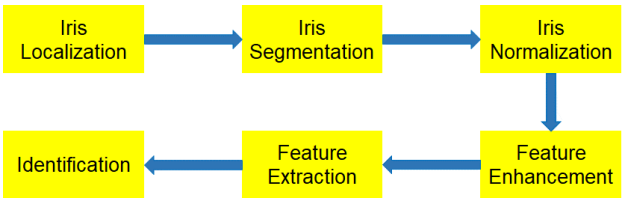

Fig. 2. Flow of the general iris recognition system.

In a traditional algorithm–based iris recognition system, the key steps are iris localization and segmentation. Obtaining the precise location of the iris position is essential, and noise removal during image segmentation increases the quality of the iris region of interest, which in turn influences system performance (Fig. 3).

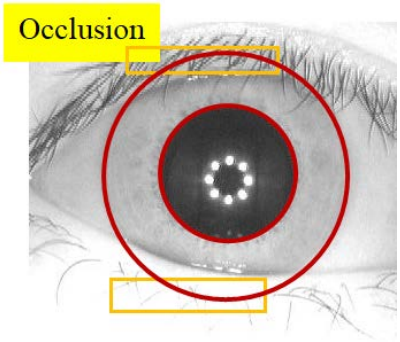

Fig. 3. Iris image.

B. Iris Identification Using Deep Learning

The computing power of Central Processing Units (CPU) and Graphics Processing Units (GPU) has improved considerably, greatly contributing to deep learning. With such developments, many iris recognition systems based on machine learning and deep learning have been implemented. Regardless of whether an iris recognition system is based on machine learning or deep learning, the recognition procedure is similar to that of traditional iris recognition systems. In Ref. [22], the study used CNN-based technology for iris recognition. When the iris region is obscured for authentication, this study focused on the ocular region along with the periocular region for biometric authentication. Due to iris segmentation, image blurring, contouring and partial occlusion by eyelids and eyelashes, the periocular region offers higher detection rates compared to the performance of iris detection algorithms in difficult imaging conditions. In Ref. [23], previous iris recognition methods cannot effectively extract local texture features in low-resolution application scenarios, resulting in poor recognition accuracy, and the study proposed DBANet, a novel two-branch attentional deep neural network for biological iris recognition that can achieve high fidelity in both high- and low-resolution images. In Ref. [24], unrestricted iris biometrics has become even more popular due to diverse user applications with CNN models, and a guided CNN-based localization and segmentation approach, IrisGuideNet, was proposed in this work, which guides the network to reduce dependency on model data. This work also used the new iris infusion technology to refine the predicted output of the data, exploiting the geometric relationships between the outputs by network inference.

III. Proposed Two-Stage Deep-Learning Based Design

The iris recognition system comprises iris ROI extraction and image identification, termed the two-stage recognition method in this study. In most studies, traditional algorithms have been widely used for iris ROI extraction, and classifiers have been employed for image identification, in which normalized images are input. Iris ROI extraction was further subdivided into three steps, namely iris localization, ROI segmentation, and feature enhancement. Fig. 4 presents an overview of the two-stage recognition method. The proposed iris localization method was based on deep learning techniques, including You Only Look Once (YOLO)-based object detection. Images that did not undergo normalization were used as the input for the classifier.

YOLO is a state-of-the-art real-time object detection system developed by Joseph Redmon. A real-time object recognition system that can recognize multiple objects within an image frame. YOLO has evolved into new versions over time, e.g., YOLOv2, YOLOv3, and YOLOv4 [25]. YOLOv4 is an object detection algorithm that evolves the YOLOv3 model. It is twice as fast as EfficientDet and has comparable performance. Moreover, the performances for average accuracy and frames per second of YOLOv4 are increased compared to YOLOv3. YOLOv4-tiny [25, 26] is a compressed version of YOLOv4. Based on YOLOv4, it is proposed to simplify the network structure, reduce parameters and enable development on embedded devices, and YOLOv4-tiny based model performs faster training and faster detection by comparison with YOLOv4. For real-time object detection and location, YOLOv4-tiny is a better option when compared to YOLOv4. This is because when using real-time object detection, faster inference time is more important than accuracy.

A. YOLO-Based Iris Localization

Fig. 4 depicts the flow of the two-stage recognition method based on deep learning. First, with the deep learning model, i.e., an YOLOv4-tiny based object detector, was employed to perform iris and pupil localization. The algorithm was then applied to obtain the exact position and radius of the pupil and iris. Second, the iris ROI was then segmented according to this information; five different methods were applied. Third, features were enhanced through image processing, and finally, the image was identified using EfficientNet, i.e., a deep learning based classifier.

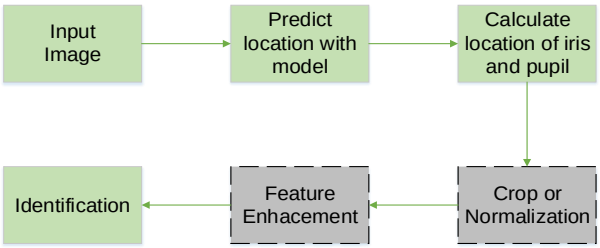

Fig. 4. Two-stage processing flow.

In this study, we propose a method for iris localization based on deep learning object detection. YOLOv4-tiny, i.e., the fastest object detector, was adapted to reduce time and space complexity owing to its smaller model size. Although the semantic segmentation model [27, 28], which provides a label for each pixel, more precisely segments each target boundary than does an object detector, the model size is large and image prediction is more time-consuming. Table I describes the comparison of different iris localization methods. The YOLOv4-tiny model detects the iris and pupil location in each image but has two shortcomings, namely deviation from the bounding box and error prediction (Fig. 5(a)–5(d)).

TABLE I. Comparison of Different Iris Localization Methods

Iris Localization	Advantage	Disadvantage
Semantic Segmentation of Iris [27]	Complete iris information	The complexity of algorithm after iris localization is higher
Semantic Segmentation of Pupil [28]	The complexity of algorithm after iris localization is lower	Incomplete iris information
Proposed YOLO Based Iris Localization	The complexity of model is the lowest	Iris information contain noises

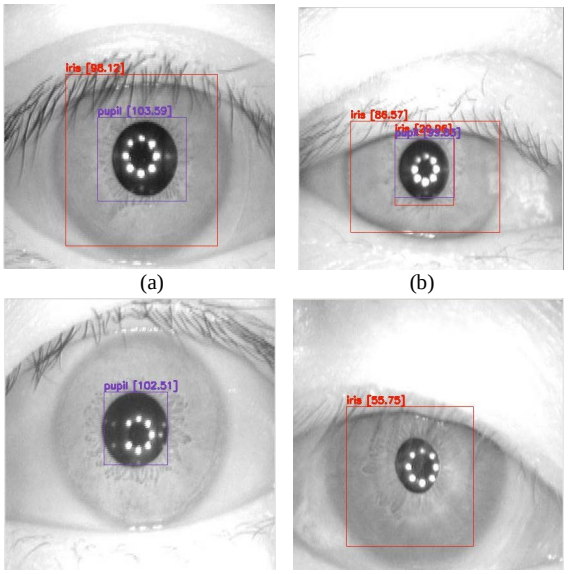

Fig. 5. Detection of iris and pupil locations by YOLOv4-tiny model. (a) Deviation of the bounding box (b) Multiple bounding boxes for the same target (c) Pupil bounding box only (d) Iris bounding box only.

With regard to bounding box deviation, the iris ROI includes too much noise, and with error prediction, multiple bounding boxes in different sizes and locations may be predicted for the same object. To solve the first problem, the bounding box must be precisely placed to carefully align with the iris or pupil boundary to reduce deviation during image labeling. To address the second problem, the amount of anchor boxes must be reduced because too many can create multiple bounding boxes. The output layer of the YOLOv4-tiny model is the detection layer, and each pixel on the feature map of detection layer is called a cell. Each cell predicts the corresponding bounding boxes according to the anchor boxes. For example, if three anchor boxes are used for the output layer, each cell predicts three bounding boxes. In this method, only the two classes of iris and pupil must be detected. An excessive number of anchor boxes increases the probability of generating multiple bounding boxes for the same target. As a result, we used only two anchor boxes to detect the object. Furthermore, small-scale image detection was abandoned on account of the large size of the bounding box after clustering.

To further solve problems related to this model, The algorithm process was divided into target bounding box selection and iris ROI extraction. The predicted bounding box of the YOLO model can be divided into the following three scenarios: (1) One iris and one pupil bounding box, (2) the generation of excessive bounding boxes of the same target when both iris and pupil bounding boxes are used, and (3) only one iris bounding box. For the first case, if one iris bounding box and pupil bounding box are respectively generated, whether the pupil bounding box is inside the iris bounding box must be confirmed; if this is the case, these two bounding boxes are our target (Fig. 5(a)); otherwise, this image is discarded. Regarding the second case (Fig. 5(b)), the size of the different object bounding boxes must be assessed when excessive bounding boxes of the same target are generated. If the size and center position of the pupil and iris bounding boxes are similar, the iris bounding box is discarded because this one is more likely to be erroneously detected during experiments. Subsequently, the Euclidean distance between all iris and pupil bounding boxes is calculated, and those with the smallest Euclidean distance are designated as target bounding boxes. In terms of the last scenario, if only one pupil bounding box is generated, the iris and pupil are considered to be concentric circles (Fig. 5(c)), and the iris radius is assumed to be equal to the pupil radius plus 50 pixels. For scenarios not described, the images can be removed and then regarded as images of intruders.

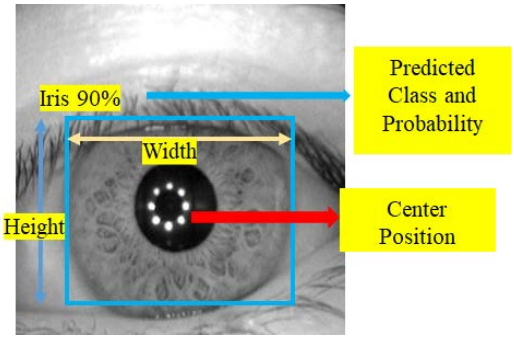

Fig. 6. Bounding box information.

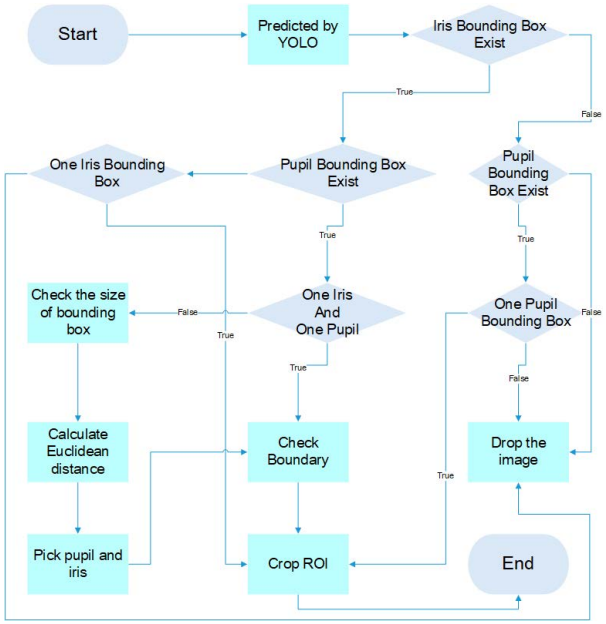

Fig. 7. Flowchart of YOLOv4-tiny based iris localization.

After selection of the target bounding box, the iris ROI is extracted. To prevent noise, the following process is performed. First, the radii of the pupil and iris are obtained from the bounding box information predicted by the YOLOv4-tiny model, which contains center position, height, width, and predicted class (Fig. 6). To calculate the real size of the target, we compared the height and width, with the smaller value selected as the radius. If the larger value was used as the radius of the circle, too much noise would be included. After selection of the radius, the radius is expanded by multiplying the parameter by 1.2;

thus, no pupil information is contained in the ROI. The parameter 1.2 is calculated from the image of the dataset. The center of the circle is the center position of the bounding box. Finally, information on the pupil circle and iris circle is used to extract the iris ROI. Fig. 7 presents the flowchart of YOLOv4-tiny based iris localization, and Table II depicts image lists after image normalization and enhancement by YOLOv4-tiny based iris localization.

TABLE II. IMAGE LIST FOR YOLOV4-TINY BASED IRIS LOCALIZATION

	NonFE	Histogram Equalization	CLAHE	Gabor
Uncropped				
Cropped with Pupil	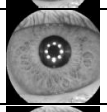	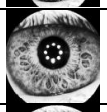	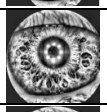	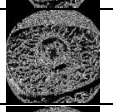
Cropped without Pupil	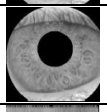		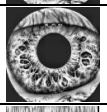	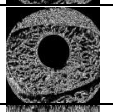
Circular Normalization	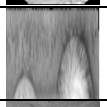	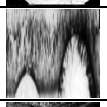		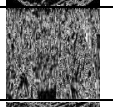
Side Normalization	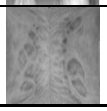		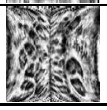	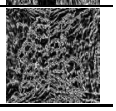

IV. EXPERIMENTAL RESULTS AND COMPARISONS

A. Datasets

In this study, images from 249 people were collected from CASIA-v3, or called CASIA-IrisV3 for short (Fig. 8) to form the data set [29]. In Ref. [29], CASIA-IrisV3 includes a total number of 22,035 iris images from over 700 persons, and all iris images are 8-bit grayscale JPEG files. All images in this data set were near-infrared (NIR) illumination images instead of visible images in consideration of their practical application. Each subset collected from an individual in this data set was divided into training, validation, and testing subsets at a fixed ratio of 8:1:1 to account for the varying number of images from each person. For experiments, the used computer platform includes a CPU by Intel Core i9-10980XE, a GPU by NVIDIA RTX2080Ti, and the 32 GB RAM size.

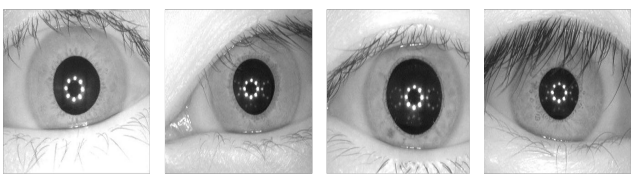

Fig. 8. Images from CASIAv3 (Available: http://biometrics.idealtest.org/).

B. Evaluation Indexes

To assess the performance of the model, evaluation indexes calculated using a confusion matrix were used. Each evaluation index was rigorously selected according to the model. In statistics, a False Positive (FP) is also known as a Type I error, and a False Negative (FN) is a Type II error. Certain statistical theories are dedicated to the minimization of these errors in different situations. For an access control system, false positives (Type I errors) are expected to be eliminated; otherwise, safety could be affected. However, to identify terrorists, the elimination of false negatives (Type II errors) is paramount because of the potential threat that arises when a terrorist is not detected. Therefore, different evaluation indexes are required based on a system's purpose. Evaluation indexes used in this study included accuracy, False Acceptance Rate (FAR), False Rejection Rate (FRR), and Equal Error Rate (EER) [30] (Fig. 9). Equal Error Rate (EER) is a metric used in biometric security systems to measure the system's effectiveness in correctly identifying individuals. The EER is the point at which the False Acceptance Rate (FAR) equals the False Rejection Rate (FRR). Accuracy is widely used in general models but is not intuitive when the numbers of data for each ground truth are uneven. To evaluate the performance of the access control system. The FAR and FRR were adjusted using the threshold value and probability of prediction. The FAR is the probability of access by unauthorized people, and the FRR is the probability of system rejection for authorized people. If the threshold of the system is too low, the FAR increases, which may comprise safety in these types of systems. By contrast, if the threshold is too high, the FRR increases, and those deserving of access could be easily rejected by the system. Thus, an appropriate threshold for the system, represented by the EER, is crucial.

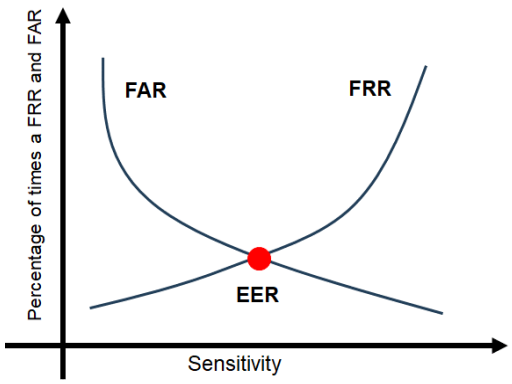

Fig. 9. EER [32] (Available: https://www.recogtech.com/en/knowledge-base/security-level-versus-user-convenience).

C. System Safety Analysis

This experiment tested the safety of the entire system, that is, whether intruders were correctly rejected by the system. Images collected from 80 people were selected from the data set, half of which were used as the training data set for the recognition model based on EfficientNet; the other images were designated as intruder images and

used to verify the safety of the system. A performance-based comparison of different methods combines iris localization, iris normalization, and feature enhancement. Compared with the one-stage model [31, 32], the two-stage model's recognition methods obtained much lower EER values.

Notably, the experiment revealed that feature enhancement of images was not necessary for the model that used the classifier to identify images, and system performance was affected by feature enhancement. Among them, the Gabor filter obtained the least effective performance despite exhibiting a slightly lower EER value when the images were normalized. Table III lists the EER by the proposed YOLOv4-tiny based iris localization technology.

TABLE III. EER OF YOLOV4-TINY BASED IRIS LOCALIZATION

EER	NonFE	Histogram Equalization	CLAHE	Gabor
Uncropped	~0%	1.92%	~0%	0.99%
Cropped with Pupil	~0%	2.04%	2.04%	12.24%
Cropped without Pupil	~0%	~0%	~0%	~0%
Circular Normalization	~0%	~0%	~0%	4.08%
Side Normalization	~0%	~0%	~0%	~0%

D. System Affordability Analysis

In this part of the study, the system's affordability was analyzed and its performance evaluated using the accuracy index. The data set images, collected from 249 people, were trained together to analyze the extent to which the performance of the system was affected by the number of imaged individuals.

Table IV lists the accuracy by the proposed YOLOv4-tiny based iris localization technology. In iris localization by the YOLOv4-tiny model with the pupil and iris boundaries, the predicted images with less noise, such as from eyelids and eyelashes, achieved high accuracy. The experimental evidence for ROI segmentation shows that on average, experiments with cropped images, regardless of the availability of pupil information, outperformed those without cropped images. In experiments, to attain better performance in ROI segmentation, the black background and pupil must be discarded but normalization is unnecessary. By comparisons, feature enhancement seems to be not required for recognition systems, either for safety or affordability. The differences among the proposed design and that of other experiments reported in [19, 20] are described in Table V; the accuracy of the proposed design was higher. In addition, the iris ROI can be segmented more precisely because the proposed design was susceptible to interference from eyelashes and eyelids during segmentation.

TABLE IV. ACCURACY OF YOLOV4-TINY BASED IRIS LOCALIZATION

Accuracy	NonFE	Histogram Equalization	CLAHE	Gabor
Uncropped	97.95%	96.59%	96.59%	93.86%
Cropped with Pupil	97.61%	97.61%	92.15%	83.62%
Cropped without Pupil	97.95%	97.61%	97.61%	96.25%
Circular Normalization	97.61%	97.61%	71.67%	78.16%
Side Normalization	96.93%	96.93%	87.03%	95.22%

TABLE V. COMPARISON AMONG THE RELATED DESIGNS

	Design in [19]	Design in [20]	Proposed method
Database	CASIA Iris Interval	CASIA-v4 Lamp	CASIA-v3
Number of People	90	822	249
Accuracy	96.67%	93.87%	~98%

V. CONCLUSION

In this study, two-stage deep-learning-based iris recognition methods were developed for biometric authentication on small community. The proposed methods can be used to enhance safety in daily life. The procedures were divided into iris localization, segmentation, and identification. For iris localization, YOLOv4-tiny, the fastest object detector model, determined the iris location with little noise and within a relatively short time. With regard to iris segmentation, iris normalization was optional when it was implemented in the iris recognition system with the classifier based on deep learning. The iris recognition system became more stable when the pupil information and background were removed from the images. In addition, images without feature enhancement achieved the best results in the experiments, indicating that feature enhancement is optional for the classifier. In summary, the proposed biometric authentication is consisted of YOLOv4-tiny based location of pupil, cropped without pupil and the image without feature enhancement. Besides, the image without normalization reach higher accuracy in the experimental results.

CONFLICT OF INTEREST

The authors declare no conflict of interest.

AUTHOR CONTRIBUTIONS

Cheng-Shun Hsiao conducted the research and wrote the paper. Chia-An Chang analyzed the data. This paper was revised by Chih-Peng Fan. All authors had approved the final version.

FUNDING

This work was financially supported partly by the National Science and Technology Council under Grant No. NSTC 111-2218-E-A49-028.

REFERENCES

[1] N. T. Hoan, L. T. Thuong, and N. D. Thang, "Multiple watermarking with biometric data using discrete curvelets and contourlets," *Journal of Image and Graphics*, vol. 6, No. 2, pp. 122–126, December 2018. doi: 10.18178/joig.6.2.122-126

[2] R. Ryu, S. Yeom, S. H. Kim, and D. Herbert, "Continuous multimodal biometric authentication schemes: A systematic review," *IEEE Access*, vol. 9, pp. 34541–34557, 2021.

[3] J. G. Daugman, "High confidence visual recognition of persons by a test of statistical independence," *IEEE Transactions on Pattern Analysis* and *Machine Intelligence*, vol. 15, no. 11, pp. 1148–1161, Nov. 1993. doi: 10.1109/34.244676

[4] Q. C. Tian, Q. Pan, Y. M. Cheng, and Q. X. Gao, "Fast algorithm and application of Hough transform in iris segmentation," in *Proc. 2004 International Conference on Machine Learning and*

Cybernetics (IEEE Cat. No.04EX826), 2004, pp. 3977–3980. doi: 10.1109/ICMLC.2004.1384533

[5] F. R. J. López, C. E. P. Beainy, and O. E. U. Mendez, "Biometric iris recognition using Hough transform," in *Proc. Symposium of Signals, Images and Artificial Vision: STSIVA 2013*, Bogota, 2013, pp. 1–6. doi: 10.1109/STSIVA.2013.6644905

[6] W. J. Ryan, D. L. Woodard, A. T. Duchowski, and S. T. Birchfield, "Adapting starburst for elliptical iris segmentation," in *Proc. 2008 IEEE Second International Conference on Biometrics: Theory, Applications and Systems*, 2008, pp. 1–7. doi: 10.1109/BTAS.2008.4699340

[7] M. Happold, "Structured Forest edge detectors for improved eyelid and iris segmentation," in *Proc. 2015 International Conference of the Biometrics Special Interest Group (BIOSIG)*, 2015, pp. 1–6. doi: 10.1109/BIOSIG.2015.7314622

[8] G. Qiaoli, H. Cao, D. Benqing, and Z. Xiang, "The iris normalization method based on line," in *Proc. 2013 Fourth International Conference on Intelligent Systems Design and Engineering Applications*, 2013, pp. 669–671. doi: 10.1109/ISDEA.2013.559

[9] A. Mohammed and M. F. Al-Gailani, "Developing iris recognition system based on enhanced normalization," in *Proc. 2019 2nd Scientific Conference of Computer Sciences (SCCS)*, 2019, pp. 167–170. doi: 10.1109/SCCS.2019.8852622

[10] A. I. Ismail, H. S. Ali, and F. A. Farag, "Efficient enhancement and matching for iris recognition using SURF," in *Proc. 2015 5th National Symposium on Information Technology: Towards New Smart World (NSITNSW)*, 2015, pp. 1–5. doi: 10.1109/NSITNSW.2015.7176409.

[11] D. G. Lowe, "Distinctive image features from scale invariant keypoint," *International Journal of Computer Vision*, pp. 1–28, January 2004.

[12] H. Bay, T. Tuytelaars, and L. Gool, "Surf: Speeded up robust features," in *Proc. European Conference on Computer Vision*, May 2006, pp. 404–417.

[13] O. Koç and A. Uka, "A new encoding of iris images employing eight quantization levels," *Journal of Image and Graphics*, vol. 4, No. 2, pp. 78–83, December 2016. doi: 10.18178/joig.4.2.78-83

[14] A. N. Ali, "Simple features generation method for SVM based iris classification," in *Proc. 2013 IEEE International Conference on Control System, Computing and Engineering*, 2013, pp. 238–242. doi: 10.1109/ICCSCE.2013.6719966

[15] Y. Bouzouina and L. Hamami, "Multimodal biometric: Iris and face recognition based on feature selection of iris with GA and scores level fusion with SVM," in *Proc. 2017 2nd International Conference on Bio-engineering for Smart Technologies (BioSMART)*, 2017, pp. 1–7. doi: 10.1109/BIOSMART.2017.8095312

[16] M. Sardar, S. Banerjee, and S. Mitra, "Iris segmentation using interactive deep learning," *IEEE Access*, vol. 8, pp. 219322–219330, 2020. doi: 10.1109/ACCESS.2020.3041519

[17] C. Wang, J. Muhammad, Y. Wang, Z. He, and Z. Sun, "Towards complete and accurate iris segmentation using deep multi-task attention network for non-cooperative iris recognition," *IEEE Transactions on Information Forensics and Security*, vol. 15, pp. 2944–2959, 2020. doi: 10.1109/TIFS.2020.2980791

[18] S. Thakkar and C. Patel, "Iris recognition supported best gabor filters and deep learning CNN options," in *Proc. 2020 International Conference on Industry 4.0 Technology (I4Tech)*, 2020, pp. 167–170. doi: 10.1109/I4Tech48345.2020.9102681

[19] L. T. Thuong, P. X. Hanh, N. D. Phu, and L. B. Loc, "Iris-based biometric recognition using modified convolutional neural network," in *Proc. 2018 International Conference on Advanced Technologies for Communications (ATC)*, 2018, pp. 184–188. doi: 10.1109/ATC.2018.8587560

[20] T. Zhao, Y. Liu, G. Huo, and X. Zhu, "A deep learning iris recognition method based on capsule network architecture," *IEEE Access*, vol. 7, pp. 49691–49701, 2019. doi: 10.1109/ACCESS.2019.2911056

[21] D. Li, C. Wu, and Y. Wang, "A novel iris texture extraction scheme for iris presentation attack detection," *Journal of Image and Graphics*, vol. 9, no. 3, pp. 95–102, September 2021. doi: 10.18178/joig.9.3.95-102

[22] N. Prasanth, C. U. S. Kiran, S. Nethi, T. Ketineni, N. Srinivasu, and G. Pradeepini, "Fusion of iris and periocular biometrics authentication using CNN," presented at 2023 7th International Conference on Computing Methodologies and Communication (ICCMC), Erode, India, 2023.

[23] J. Chen, Y. Cui, F.Shen, J. Shen, and T. Wei, "DBANet: A dual branch attention-based deep neural network for biological iris recognition," presented at 2022 IEEE International Conference on Bioinformatics and Biomedicine (BIBM), Las Vegas, NV, USA, 2022.

[24] J. Muhammad, C. Wang, Y. Wang, K. Zhang, and Z. Sun, "IrisGuideNet: Guided localization and segmentation network for unconstrained iris biometrics," *IEEE Transactions on Information Forensics and Security*, vol. 18, pp. 2723–2736, 2023.

[25] D. Zhu, G. Xu, J. Zhou, E. Di, and M. Li, "Object detection in complex road scenarios: Improved YOLOv4-tiny algorithm," presented at 2021 2nd Information Communication Technologies Conference (ICTC), Nanjing, China, 2021.

[26] Y. Shi, Z. Gao, and S. Li, "Real-time detection algorithm of marine organisms based on improved YOLOv4-tiny," *IEEE Access*, vol. 10, December 2022.

[27] C. S. Hsiao, C. P. Fan, and Y. T. Hwang, "Design and analysis of deep-learning based iris recognition technologies by combination of U-Net and EfficientNet," presented at 9th International Conference on Information and Education Technology (ICIET 2021), Okayama, Japan, 2021.

[28] C. S. Hsiao and C. P. Fan, "EfficientNet based iris biometric recognition methods with iris positioning by U-Net," in *Proc. The 3rd International Conference on Computer Communication and the Internet (ICCCI 2021)*, 2021, pp. 1–5.

[29] Chinese Academy of Sciences Institute of Automation. CASIA Iris Image Database. [Online]. Available: http://www.cbsr.ia.ac.cn/IrisDatabase.htm

[30] Equal Error Rate (EER). [Online]. Available: http://Wikipedia/Biometrics

[31] C. W. Chuang and C. P. Fan, "Biometric authentication with combined iris and sclera information by YOLO-based deep-learning network," in *Proc. 2020 IEEE International Conference on Consumer Electronics - Taiwan (ICCE-Taiwan)*, 2020, pp. 1–2. doi: 10.1109/ICCE-Taiwan49838.2020.9258253

[32] C. W. Chuang, C. P. Fan, and R. C. H. Chang, "Design of low-complexity YOLOv3-based deep-learning networks with joint iris and sclera messages for biometric recognition application," in *Proc. 2020 IEEE 9th Global Conference on Consumer Electronics (GCCE)*, 2020, pp. 150–151. doi: 10.1109/GCCE50665.2020.9291805